Graphene Edges and Beyond: Temperature-Driven Structures and Electromagnetic Properties

Changbae Hyun,[†,¶] Jeonghun Yun,[†,∥,¶] Woo Jong Cho,[†] Chang Woo Myung,[†] Jaesung Park,[⊥] Geunsik Lee,[†] Zonghoon Lee,[§] Kwanpyo Kim,[‡] and Kwang S. Kim*[,†,‡]

[†]Department of Chemistry, [‡]Department of Physics, and [§]Department of Materials Science and Engineering, Ulsan National Institute of Science and Technology (UNIST), Ulsan 689-798, Korea, [∥]Department of Chemistry, Pohang University of Science and Technology, Pohang 790-784, Korea, and [⊥]Center for Electricity & Magnetism, Korea Research Institute of Standards and Science, Daejeon 305-340, Korea. [¶]C.H. and J.Y. contributed equally.

ABSTRACT The atomic configuration of graphene edges significantly influences the various properties of graphene nanostructures, and realistic device fabrication requires precise engineering of graphene edges. However, the imaging and analysis of the intrinsic nature of graphene edges can be illusive due to contamination problems and measurement-induced structural changes to graphene edges. In this issue of *ACS Nano*, He *et al.* report an *in situ* heating experiment in aberration-corrected transmission electron microscopy to elucidate the temperature dependence of graphene edge termination at the atomic scale. They revealed that graphene edges predominantly have zigzag terminations below 400 °C, while above 600 °C, the edges are dominated by armchair and reconstructed zigzag edges. This report brings us one step closer to the true nature of graphene edges. In this Perspective, we outline the present understanding, issues, and future challenges faced in the field of graphene-edge-based nanodevices.

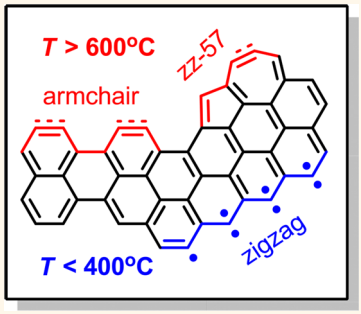

Since the first evidence of graphene as a two-dimensional (2D) material was reported, graphene has attracted extensive attention as a promising material with the extraordinary 2D nature of its electronic properties.[1] The study of graphene was further accelerated after chemical vapor deposition (CVD) graphene growth and transfer processes were reported.[2] The electronic band structure of graphene shows the Dirac cone feature near its Fermi level and results in high carrier mobility, a property that makes graphene emerge as a potential replacement for silicon electronics. When a bulk crystal becomes a thin film, the exposed surface becomes a key factor for its electronic properties, and equally, the one-dimensional (1D) edge structure in these nanosized 2D materials determines the optical and electronic properties.[3] Figure 1 shows the most typical graphene edge configurations. The electrical, magnetic, and chemical properties of graphene nanostructures, in particular, graphene nanoribbons (GNRs), are deeply rooted in the detailed atomic configuration of the edges.[4−6] Theoretical simulations predict that the armchair edge is 1.1 eV/atom more stable than the zigzag edge in the absence of any passivation. This relative stability of the armchair edge is ascribed to the self-passivation *via* singlet coupling of the dangling bonds at the armrest carbon atoms, which results in an array of benzyne-like triple-bond structures. The dangling bonds at the zigzag edge cannot be stabilized in the same way due to their spatial separation. Instead, the zigzag (zz) edge can undergo spontaneous reconstruction to the 5−7 zz (zz-57) edge, which is as stable as the armchair edge. The reconstruction takes place by Stone−Wales bond alteration, for which an energy barrier of ∼0.6 eV has to be overcome.

Edge-dependent properties were studied through engineering crystallographic orientation of graphene edges. They can be controlled by the bottom-up process of surface-assisted molecular assembly.[7] Top-down fabrication of the edge includes electron-beam lithography of CVD-grown graphene, exfoliation of graphite, scanning tunneling microscopy (STM) tip-assisted nanostructure formation, and transmission electron microscopy (TEM) electron-beam sputtering. Both STM and Raman spectroscopy

* Address correspondence to kimks@unist.ac.kr.

Published online May 26, 2015
10.1021/acsnano.5b02617

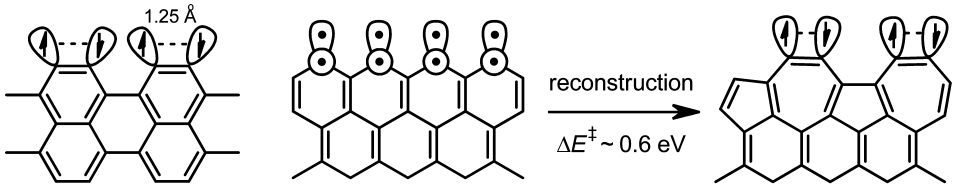

Figure 1. Typical graphene edges and their energetics. The formation energy of each edge with respect to the pristine graphene is given. Singlet coupling of dangling bonds for armchair and 5−7 zigzag (zz-57) edges is represented with dotted lines between neighboring half-filled sp^2 lobes. For the zigzag edge, the dangling bonds and π edge states are denoted by half-filled sp^2 and p lobes, respectively. The reconstruction process of zigzag edges to zz-57 edges is denoted with an arrow, where the activation energy barrier $\Delta E^{\ddagger}$ is given alongside. The calculated energy values are taken from ref 4.

techniques were previously utilized to tackle important questions on graphene edges, such as selective electronic and optical scattering processes at specific graphene edge configurations.[3,8] However, imaging of graphene edges with true atomic resolution has been challenging with the limited spatial resolution power of these instruments. With regard to this research effort, aberration-corrected transmission electron microscopy (AC-TEM) is a key instrument as it can visualize graphene edge structures even at low acceleration voltages; individual carbon atoms at graphene edges can be imaged.[9] In addition, an atomic-scale dynamic process can be explored with the temporal resolution of these instruments, which provides valuable insight into the energetics and stability of graphene edges, as well as defect formation mechanisms and structure−property relationships.

By using AC-TEM, some faces of the graphene edges at various conditions have been resolved, as shown in Figure 2. For example, the exposed graphene edge from an etched hole was monitored, revealing single-atom-level dynamics.[9] Theoretically predicted reconstructed zz-57 edges and reversible transformations between zz-57 and simple zz edge configurations were observed with the aid of electron-beam perturbation.[10] A previous study suggested that, at high temperatures, the armchair edge is the most prevalent edge structure among various edge configurations.[11]

Graphene Edge Structures. Although many studies have included TEM imaging of graphene edges, observing the true faces of graphene edges can be elusive. This challenge is related to subtle aspects with regard to TEM imaging. The first issue is the electron-beam energy for the atomically thin surfaces. Transmission electron microscopy relies on high-energy electrons passing through the sample to image the internal atomic structure, which can alter the specimens and significantly influence the structures. Although it is not possible to remove electron-beam-induced alteration fully during TEM imaging, this issue can be partly addressed if the imaging conditions and irradiation damage mechanism are known. For example, some intrinsic properties of graphene edges, such as edge energetics, can be retrieved.[10] Another important issue is the contamination of the sample. Graphene edges are typically far from ideal or pristine structures and suffer from atomic-scale defects with unintended chemical contamination. This contamination can induce nonideal behavior under an electron beam; therefore, the image can sometimes be misleading unless the contamination issue is well-addressed. As a result, it is not straightforward to draw conclusions by relying on a couple of TEM snapshots of usual graphene edges.

Girit *et al.* reported that they observed more zigzag edges than armchair edges in a graphene hole using AC-TEM with an 80 keV electron beam at room temperature.[9]

Although many studies have included transmission electron microscopy imaging of graphene edges, observing the true faces of graphene edges can be elusive.

They proposed an explanation to the apparent stability of the zigzag edge, taking into account the effects of sputtering by the electron beam. According to their explanation, the armchair edge is different from a zigzag edge in that it leaves a dangling carbon atom bonded to just one neighbor upon the knock-out of an outermost atom. Assuming that this dangling carbon atom quickly migrates away due to its instability, ejection of one atom results in the loss of two atoms for armchair edges. Therefore, the number of carbons needed to fix a vacancy is one for a zigzag edge and two for an armchair edge. As appealing as it sounds, this explanation has been challenged by subsequent studies. For example, one would expect a higher migration rate of carbon atoms when the temperature is increased or a stronger electron beam is employed. According to this explanation, these dynamics would further destabilize the armchair edge. In contrast, Song *et al.* observed that the

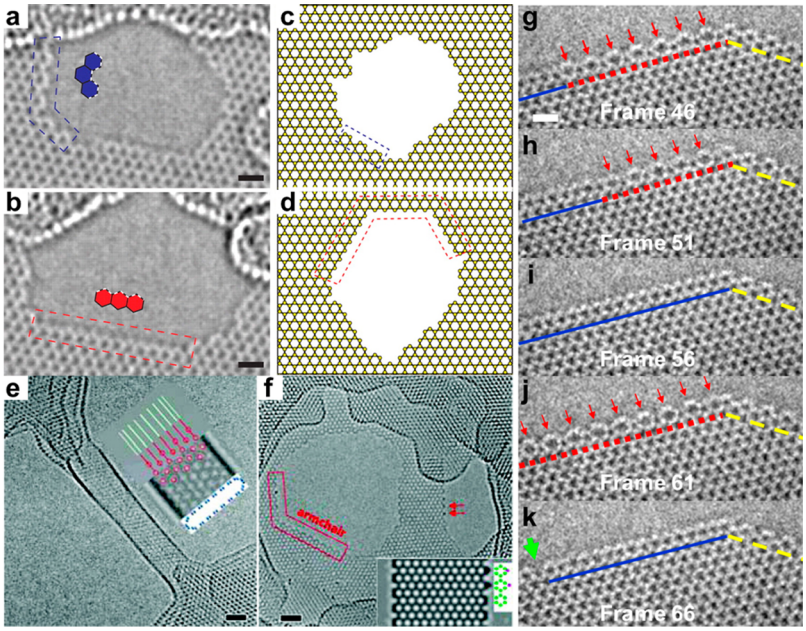

Figure 2. Examples of atomic-resolution images of graphene edges. Aberration-corrected transmission electron microscopy image of (a) an armchair (ac) and (b) zigzag (zz) configuration of carbon atoms at the edge of a hole in graphene. Scale bar, 0.5 nm. (c,d) Examples of the emergence of long-range order in the simulation of hole growth, showing (c) ac edges and (d) zz edges. Reprinted with permission from ref 9. Copyright 2009 American Association for the Advancement of Science. (e) Flat nanotube made from a few layers of graphene with high-temperature annealing. The inset shows the inferred tube shape with the high resolution TEM image and the observed (red) and estimated (green) hexagon positions for a round tube. Blue dots in the side view represent individual carbon atoms. Scale bar, 1 nm. (f) Nanoribbon made from a single layer of graphene by high-temperature annealing. The edges of the nanoribbon and the two holes are ac shaped. The inset shows the image simulation of two carbon adatoms attached to the graphene ac edges, indicated by the red arrows. Scale bar, 1 nm. Reprinted from ref 11. Copyright 2011 American Chemical Society. (g−k) Time series of TEM images of the graphene edge obtained by ripping under vacuum. Scale bar, 0.5 nm. The red arrow indicates a heptagon ring. The blue solid and red dotted lines represent zz-66 and reconstructed zz-57 edges, respectively. The yellow dashed lines show ac edge configuration. The green arrow in k shows a vacancy defect. Reprinted with permission from ref 10. Copyright 2013 Nature Publishing Group.

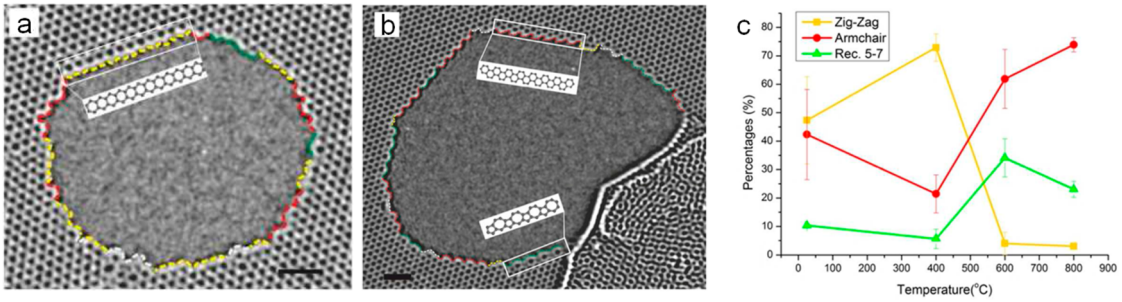

Figure 3. Graphene edge configurations at various temperatures. High-resolution transmission electron microscopy images of graphene holes at (a) room temperature and (b) 800 °C. Color-coded edges to differentiate the types of edge configuration (red, ac; yellow, zigzag; green, reconstructed 5−7 zigzag; white, mixed or unidentified edge types). All scale bars are 1 nm. (c) Temperature dependence of different edge configurations. Reprinted from ref 13. Copyright 2015 American Chemical Society.

armchair edge is more stable if the experiment is conducted with a 300 keV electron beam at 700 °C, while being able to reproduce Girit *et al.*'s result.[11] Shortly after these studies, a first-principles molecular dynamics study on the stability of graphene edges under electron-beam irradiation appeared.[12] The simulation predicts that the minimum kinetic energy transfer required to displace an edge atom without immediate recombination is 19.0 eV for the armchair edge and 12.0 eV for the zigzag edge, demonstrating the relative stability of the armchair edge under electron-beam irradiation. These findings suggest that the zigzag edge might be a kinetically favored metastable state that can persist under relatively mild conditions, and that temperature plays an important role in determining the dominant type of graphene edge.

In this issue of *ACS Nano*, He *et al.* report an *in situ* heating experiment in an AC-TEM to elucidate the temperature dependence of graphene edge terminations at the atomic scale.[13] They demonstrate that edges show predominantly 6−6 zz (zz-66) termination below 400 °C, while graphene edges display armchair (ac)

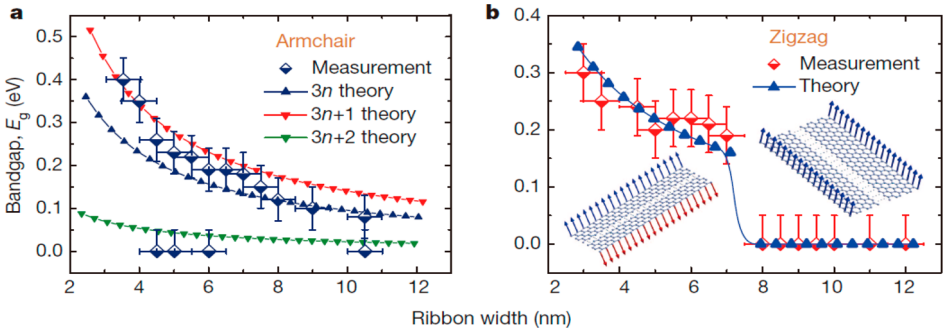

Figure 4. Edge-specific electronic and magnetic properties of graphene nanoribbons. The band gaps measured by scanning tunneling microscopy as a function of ribbon width in (a) armchair and (b) zigzag ribbons. The band structure of zigzag ribbons is governed by the emerging edge magnetism, and a sharp semiconductor (antiferromagnetic) to metal (ferromagnetic) transition is revealed. Theoretical data points were based on the mean field Hubbard model. Reprinted with permission from ref 19. Copyright 2014 Nature Publishing Group.

and reconstructed zz-57 edges above 600 °C (Figure 3). The observed dramatic transformation of edges between 400 and 600 °C can be explained by cleaning the graphene membrane by thermal annealing and increased flipping rates with increased thermal energy. At higher temperatures, the flipping between zz-57 and usual zz configurations can be thermally induced in association with electron-beam-induced energy transfer. Although previous studies gave some clues into this behavior, He *et al.* demonstrate the temperature dependence of these different edge configurations. At higher temperatures, chemical etching from sample contamination can be significantly reduced, and the observed data represent the true relative stability between the different edge configurations. Indeed, the experimental observations agree well with theoretical calculations at high temperature, but the phenomena at low temperatures will not be clear until the contamination issue is properly resolved.

Electromagnetic Properties of Graphene Edges. The electromagnetic properties of graphene edges, especially in GNRs, have been intensely investigated. The band gap of the standard armchair GNR (AGNR) decreases as the width increases, and the $3n + 2$ AGNR is predicted to be metallic in a tight-binding scheme. The zigzag GNR (ZGNR) is an antiferromagnetic semiconductor. Theoretical calculations also address the significant modification of edges.[14] For instance, ZGNR with zz-57 reconstruction modifies the electronic ground states to be singlet nonmagnetic and weakly dispersive below the Fermi level. The strong correlation effect is broken; two edge states at opposite edges hybridize slightly and break degeneracy in narrow GNRs but become degenerate for widths over 3 nm.

In this issue of *ACS Nano*, He *et al.* report an *in situ* heating experiment in an aberration-corrected transmission electron microscope to elucidate the temperature dependence of graphene edge termination at the atomic scale.

Experiments show the effects of nonuniform edges on electronic structure, which is more probable in fabrication processes. Tapasztó *et al.*[15] measured the band gaps of GNRs using STM images and scanning tunneling spectroscopy (STS). Electronic standing waves across GNR were also measured using the STM image by interpreting the interference images as electron standing wave densities. For a 10 nm wide GNR, a Fabry−Perot-like standing wave pattern across the GNR with a wavelength of 0.41 nm was observed, but for 2.5 nm width, the interference pattern was tilted 30°. This unexpected local electron density behavior demonstrates the importance of edge states for narrow GNR systems.

The role of edge states in mixed edge systems was also investigated. Ritter *et al.* used ultrahigh vacuum STM (UHV-STM) with STS to measure the local density of states on exfoliated graphene on a Si substrate.[3] A 2.3 nm wide zigzag-dominant GNR showed an energy gap smaller than that of the 2.9 nm wide AGNR. Similarly, 7−8 nm zigzag-dominant graphene quantum dots (GQDs) were metallic, and GQDs with lower fractions of zigzag edges were semiconducting.

The exotic property of ZGNRs, their antiferromagnetic ground state with the same spin aligned on each edge, has been extensively studied by first-principles calculations. Due to its possibility as a spin filter, applying bias voltages across a ZGNR was suggested based on its valence and conduction band spin orientations.[16] Giant magnetoresistance based on source and drain spin alignment was considered to be possible toward realization of spin filtering through

ZGNRs using non-equilibrium Green's function (NEGF) theory.[17]

Beyond first-principles calculations, treating ZGNRs as strongly correlated materials showed another edge magnetism effect. The Hubbard-*U* mean field approach is widely used, treating all dangling bonds in ZGNR as strongly correlated local sites. The local site interaction, *U*, is the appropriate parameter. An antiferromagnetic to ferromagnetic transition is favored in ZGNRs if accompanied by a small amount of doping per unit cell.[18] In wider ZGNRs, this transition can occur with less doping due to weakening of the edge interactions.

The ferromagnetic state in ZGNR is known to be metallic, so detecting insulator-to-metal transitions is a method of detecting antiferromagnetic-to-ferromagnetic order transitions. Recently, Magda *et al.*[19] provided experimental evidence of room-temperature ferromagnetic order combined with a theoretical explanation. Figure 4a summarizes the measured band gaps of AGNRs with theoretical predictions. A band gap caused by quantum confinement decreases inversely proportional to its width, showing overall agreement with the theoretical result. Metallic AGNRs are assumed to be $3n + 2$, which agrees with tight-binding predictions. On the other hand, Figure 4b illustrates a striking result, showing a sharp insulator-to-metal transition with increasing ZGNR width. The ZGNR width threshold was about 7 nm. Because it was assumed that this observation was evidence of a magnetic order transition from antiferromagnetic to ferromagnetic order, the result was fit with Hubbard model calculations at room temperature with $U = 3.24$ eV. Even if irregular edges, retaining dangling bonds, are assumed, the simulation still guaranteed phase transition with increased *U* of 4.32 eV.

OUTLOOK AND FUTURE CHALLENGES

Considering various capabilities of *in situ* TEM setups, the ability to monitor atomic structure and measure properties simultaneously is no longer a dream. As we described above, various physical properties of graphene nanostructures can be influenced by graphene edge structures. With the knowledge of its precise atomic edge configuration, *in situ* or *ex situ* TEM investigations can provide edge structure–property relationships. For example, by combining different structural manipulation methods, such as Joule heating and electron-beam irradiation, tailored graphene nanostructures can be investigated by electrical and thermal transport measurements. One of the big challenges in this research field is to find ways to reduce the electron-beam-induced effects for observation of intrinsic atomic structures or to take this effect into account properly in analyses. These exciting developments in AC-TEM can be utilized to investigate other nanomaterials, especially other 2D materials and related van der Waals heterostructures.[17] For example, growth of triangular holes by electron-beam irradiation on monolayer hexagonal boron nitride (hBN) was dynamically monitored over time with AC-TEM.[20] Single-atom-level dynamics revealed the mechanism of hole growth; a vacancy formed initially and grew while maintaining a triangular shape. The triangular holes persistently have nitrogen-terminated zigzag edges. The shapes and types of edges of hBN can be altered significantly at high temperatures due to charging and thermal effects of using *in situ* TEM heating. These results warrant further study of edges of hBN and other 2D materials at variable temperatures. By coupling the unprecedented resolving power of AC-TEM and *in situ* measurements with first-principles-based analyses, new research directions for addressing atomic structure–property relationships are on the horizon.

Finally, edge purity can make a big difference for ZGNR properties. In an AC-TEM environment, ZGNRs would exist in zigzag and zz-57 mixed structures, and their electronic and magnetic properties have not yet been observed. Measuring the electronic properties of partly reconstructed ZGNR, more than the band gap, could help toward understanding ZGNR properties. In addition, reconstructed zz-57 ZGNR shows its own weakly dispersive degenerate band structure; however, the degeneracy is broken in narrow ZGNRs. Investigating the orbital and band structure would help uncover the origins of ZGNR magnetic order, potentially leading toward the design of new futuristic spintronic devices.

Conflict of Interest: The authors declare no competing financial interest.

Acknowledgment. This work was supported by NRF (National Honor Scientist Program: 2010-0020414, International Research & Development Program: 2012K1A3A7A03057505) and KISTI (KSC-2014-C3-020).

REFERENCES AND NOTES

1. Novoselov, K. S.; Geim, A. K.; Morozov, S. V.; Jiang, D.; Zhang, Y.; Dubonos, S. V.; Grigorieva, I. V.; Firsov, A. A. Electric Field Effect in Atomically Thin Carbon Films. *Science* **2004**, *306*, 666–669.
2. Kim, K. S.; Zhao, Y.; Jang, H.; Lee, S. Y.; Kim, J. M.; Kim, K. S.; Ahn, J.-H.; Kim, P.; Choi, J.-Y.; Hong, B. H. Large-Scale Pattern Growth of Graphene Films for Stretchable Transparent Electrodes. *Nature* **2009**, *457*, 706–710.
3. Ritter, K. A.; Lyding, J. W. The Influence of Edge Structure on the Electronic Properties of Graphene Quantum Dots and Nanoribbons. *Nat. Mater.* **2009**, *8*, 235–242.
4. Koskinen, P.; Malola, S.; Häkkinen, H. Self-Passivating Edge Reconstructions of Graphene. *Phys. Rev. Lett.* **2008**, *101*, 115502.
5. Wassmann, T.; Seitsonen, A. P.; Saitta, A. M.; Lazzeri, M.; Mauri, F. Structure, Stability, Edge States, and Aromaticity of Graphene Ribbons. *Phys. Rev. Lett.* **2008**, *101*, 096402.
6. Son, Y. W.; Cohen, M. L.; Louie, S. G. Energy Gaps in Graphene Nanoribbons. *Phys. Rev. Lett.* **2006**, *97*, 216803.
7. Cai, J.; Ruffieux, P.; Jaafar, R.; Bieri, M.; Braun, T.; Blankenburg, S.; Muoth, M.; Seitsonen, A. P.; Saleh, M.; Feng, X.; et al. Atomically Precise Bottom-up Fabrication of Graphene Nanoribbons. *Nature* **2010**, *466*, 470–473.
8. Krauss, B.; Nemes-Incze, P.; Skakalova, V.; Biro, L. P.; von Klitzing, K.; Smet, J. H. Raman Scattering at Pure Graphene

Zigzag Edges. *Nano Lett.* **2010**, *10*, 4544–4548.
9. Girit, C. O.; Meyer, J. C.; Erni, R.; Rossell, M. D.; Kisielowski, C.; Yang, L.; Park, C.-H.; Crommie, M. F.; Cohen, M. L.; Louie, S. G.; et al. Graphene at the Edge: Stability and Dynamics. *Science* **2009**, *323*, 1705–1708.
10. Kim, K.; Coh, S.; Kisielowski, C.; Crommie, M. F.; Louie, S. G.; Cohen, M. L.; Zettl, A. Atomically Perfect Torn Graphene Edges and Their Reversible Reconstruction. *Nat. Commun.* **2013**, *4*, 2723.
11. Song, B.; Schneider, G. F.; Xu, Q.; Pandraud, G.; Dekker, C.; Zandbergen, H. Atomic-Scale Electron-Beam Sculpting of Near-Defect-Free Graphene Nanostructures. *Nano Lett.* **2011**, *11*, 2247–2250.
12. Kotakoski, J.; Santos-Cottin, D.; Krasheninnikov, A. V. Stability of Graphene Edges under Electron Beam: Equilibrium Energetics *versus* Dynamic Effects. *ACS Nano* **2012**, *6*, 671–676.
13. He, K.; Robertson, A. W.; Fan, Y.; Allen, C. S.; Lin, Y.; Suenaga, K.; Kirkland, A. I.; Warner, J. H. Temperature Dependence of the Reconstruction of Zigzag Edges in Graphene. *ACS Nano* **2015**, 10.1021/acsnano.5b01130.
14. Rodrigues, J. N. B.; Gonçalves, P. A. D.; Rodrigues, N. F. G.; Ribeiro, R. M.; Lopes Dos Santos, J. M. B.; Peres, N. M. R. Zigzag Graphene Nanoribbon Edge Reconstruction with Stone–Wales Defects. *Phys. Rev. B* **2011**, *84*, 155435.
15. Tapasztó, L.; Dobrik, G.; Lambin, P.; Biró, L. P. Tailoring the Atomic Structure of Graphene Nanoribbons by Scanning Tunnelling Microscope Lithography. *Nat. Nanotechnol.* **2008**, *3*, 397–401.
16. Son, Y.-W.; Cohen, M. L.; Louie, S. G. Half-Metallic Graphene Nanoribbons. *Nature* **2006**, *444*, 347–349.
17. Kim, W. Y.; Kim, K. S. Prediction of Very Large Values of Magnetoresistance in a Graphene Nanoribbon Device. *Nat. Nanotechnol.* **2008**, *3*, 408–412.
18. Jung, J.; MacDonald, A. H. Carrier Density and Magnetism in Graphene Zigzag Nanoribbons. *Phys. Rev. B* **2009**, *79*, 235433.
19. Magda, G. Z.; Jin, X.; Hagymási, I.; Vancsó, P.; Osváth, Z.; Nemes-Incze, P.; Hwang, C.; Biró, L. P.; Tapasztó, L. Room-Temperature Magnetic Order on Zigzag Edges of Narrow Graphene Nanoribbons. *Nature* **2014**, *514*, 608–611.
20. Ryu, G. H.; Park, H. J.; Ryou, J.; Park, J.; Lee, J.; Kim, G.; Shin, H. S.; Bielawski, C. W.; Ruoff, R. S.; Hong, S.; et al. Atomic-Scale Dynamics of Triangular Hole Growth in Monolayer Hexagonal Boron Nitride under Electron Irradiation. *Nanoscale* **2015**, 10.1039/C5NR01473E.